www.s2is.org
International Journal on Smart Sensing and Intelligent Systems
ISSN 1178-5608

WEAK GPS ACQUISITION VIA COMPRESSED DIFFERENTIAL DETECTION USING STRUCTURED MEASUREMENT MATRIX

G.Arul Elango* and Gnanou Florence Sudha

Department of Electronics and Communication Engineering,

Pondicherry Engineering College, Puducherry, India.

Email: arulelango2012@gmail.com*

Submitted: July 12, 2016 ***Accepted: Oct. 28, 2016*** ***Published: Dec. 1, 2016***

Abstract- Quality of the acquisition algorithm is the main criteria for assessment of the GPS receiver. Compressed sensing has been used recently in the GPS signal acquisition process to improve the acquisition sensitivity and find visible satellites in the two dimensional search space. In this paper, strategies for constructing the GPS Dictionary matrix using different measurement matrices are analyzed for weak signal conditions. Conventional acquisition methods use pure random or Bernoulli measurement matrices requiring huge storage memory and resulting in high computational cost for faithful sparse signal representation. Based on the restricted isometry and coherence properties, the Kronecker product of hybrid 'L' deterministic measurement matrix has been proposed for fast calculation and easy hardware implementation of the GPS acquisition module. Simulation results for weak signals of C/N_0 25 dB-Hz show that the compressed sensing combined with post-correlation differential detection scheme has the ability to determine more number of visible satellites. It is inferred that using this approach, 92% probability of obtaining 1.2 times more visible satellites than the uncompressed data length of 8 msec is achieved with lower computation time and significant improvement in average post correlation SNR value of 0.84 dB is obtained for four visible satellites.

Index terms: GPS, weak signal Acquisition, Compressed sensing, differential detection

I. INTRODUCTION

Global Positioning Systems (GPS) play a significant role in providing reliable and robust worldwide positioning for the increasing demand of location based positioning services. Signal acquisition is the first stage of the GPS receiver signal processing chain followed by tracking, bit, frame synchronization and positioning. In the acquisition stage, the naive way of finding visible satellites from the raw GPS data is based on typical serial and parallel code phase search schemes. This involves identifying the correct match in the cell, having the highest peak that cross the specified threshold value. Under weak signal conditions, the number of search steps required for both methods is quite high and sometimes this leads to reacquisition of the GPS data. Hence to alleviate signal degradation problems, a longer duration data is required to process the signal. As the processing data size increases, the number of search steps and the cell size becomes more. This results in increasing the time required to obtain the first position fix during cold start conditions. This increase influences the next stage, namely the tracking process as the tracking circuit has a very narrow bandwidth and sensitivity is relatively high in comparison with the acquisition stage. For example, to handle, 25 dB-Hz weak GPS signal, the longer duration period requires 1 msec coherent combining of 40 msec differential accumulations. Suppose the sampling frequency is set as 5.174 MHz, then the 40 msec data in a typical parallel code search acquisition require 2,28,560 FFT operations, which is very time-consuming.

Compressed sensing, a new paradigm in signal processing has acclaimed an overwhelming response in today's research as it allows the entire signal to be sampled below the Nyquist sampling rate [1]. The main aim of sparse signal processing based GPS signal acquisition is to identify the satellite visibility with lesser computation burden and this has been implemented in few literatures. Younina eldar et.al, [2] decomposes the GPS signal acquisition problem as a sparse spike representation of compressed measurement below the Nyquist rate. To enhance the Signal-to-Noise Ratio (SNR), T. L. Hansen et.al [3] proposed a rank deficient dictionary by choosing the rows of the measurement matrix as a random combination of the columns in the dictionary. To achieve higher acquisition rate in GPS signal acquisition, Ihsan Alshahib Lami et.al [4], proposed a Jacket matrix based deterministic waveform generator as a best orthogonal transform to sparsify the received weak signals in a harsh environment. Bhattacharyya et.al [5], proposed a prolate spheroidal wave function as a basis transform to recover a weak GPS signal

level of 35dB-Hz using compressed sensing approach. Prasant Misra et.al [6], implemented energy efficient GPS sensing on cloud offloading. In this work, the dictionary matrix is formed using random or Bernouli measurement matrix on the cloud server employed in smart phones to minimize the processing time and the energy to certain extent compared to the normal acquisition schemes. Moreover, the authors used 2 msec chunks of data to acquire the weak signal using compressed sensing strategy so that more number of visible satellites could be acquired with high accuracy and 5 to 10 times lower energy than a standalone GPS. But, the random measurement matrix consumes more storage and complexity while implementing in hardware. Many literatures [7-12] have dealt with formation of structured deterministic measurement matrices for faithful reconstruction of image, speech and video signal with high probability of success rate and good PSNR value. Hence, still there is a quest for designing an optimum measurement matrix with low storage requirement and complexity.

In this paper, to minimize the computational complexity in weak GPS signal acquisition, the differential compressed detection measurement using structured sensing matrix has been proposed. In this work, the sparse GPS signal is represented as a linear combination of compressed measurements with circularly shifted pseudo random noise code (PRN) bases. The measurement matrix is designed based on the Kronecker product of hybrid ‘L’ matrices. This follows a certain fixed pattern and the important properties of the compressed sensing like spark, Restricted Isometry Property (RIP) and mutual coherence have been satisfied. Simulation results demonstrate the superior performance of the proposed method in terms of increased satellite visibility at a shorter mean acquisition time and improvement in average post correlation SNR.

The remainder of the paper has been organized as given below. Section 2 describes the basics of compressed sensing. In section 3, the structure of the GPS sparse signal formulation is illustrated. The Kronecker product based ‘L ‘matrix and important properties like spark, mutual coherence and RIP are discussed. The GPS acquisition sensitivity analysis like ratio of compressed to uncompressed 20 msec segment, absolute data and execution time using structured measurement matrix is determined and compared with other measurement matrices in Section 4.

II. OVERVIEW OF COMPRESSIVE SENSING

Compressed sensing (CS) is a signal processing technique for efficiently acquiring and reconstructing a signal by finding solutions to underdetermined linear systems. Natural signals can be represented as sparse signals either in time or frequency domain with a certain basis. Sparse signals can be compressively sampled i.e., the number of samples needed for perfect reconstruction is less than that specified by the Nyquist sampling theorem [1]. A signal is said to be k-sparse if only 'k' non-zero elements are needed to represent the signal. Any sparse signal can be represented as a linear combination of basis matrix with larger number of smaller amplitude and smaller number of larger amplitude coefficients.

For example, the sparse signal x can be described mathematically as

$$x = \sum_{i=1}^{N} \psi_i \, s_i \tag{1}$$

where ψ represents the basis and s_i is the sparse co-efficient. Hence, compressed sensing includes formation of measurement matrix, basis matrix and reconstruction of sparse vector.

For sparse signal representation, the compressed measurement 'y' of the input signal vector 'x' is computed as

$$y = \phi \, x \tag{2}$$

where y is an M × 1 measurement vector, Φ is an M × N measurement matrix and M ≪ N.

Using (1), y can be rewritten as

$$y = D\,\mathrm{s} \tag{3}$$

where $D = \phi\psi$ of size M × N.

Generally, an m × n linear system is underdetermined, when there are fewer equations than the unknowns (i.e., m < n) thereby having no unique solution resulting in infinitely many solutions. The major problem associated with CS concept is to solve an underdetermined system of equations to recover the original signal x from the measurement vector y. But y is ill-posed since M < N.

In [13], to recover a sparse signal from very few non adaptive, linear measurements convex optimization is used, in which the sparest vector is computed by solving the well-known under determined problem with sparsity constraint, s = arg min $||s||_0$ subject to $y = \phi\psi s$, where $||s||_0$ denotes ℓ_0-norm that counts the number of nonzero entries in a vector. However, as this is a Non

deterministic Polynomial (NP) hard problem, the recovery of sparse vector is obtained via ℓ_1-norm minimization in [14].

III. SPARSE SIGNAL FORMULATION IN GPS ACQUISITION BY DIFFERENTIAL COMPRESSED DETECTION USING STRUCTURED SENSING MATRIX

The GPS signal is not exactly a sparse signal. The sparse structure can be formulated by performing two different sweeps, namely frequency sweep and code sweep. The problem formulation of GPS sparse signal and its recovery are shown in figure 1. After down conversion to baseband, the signal from all the satellites can be represented in complex baseband representation by (4) as in [15]

$$y(t) = \sum_{s=0}^{S-1} \alpha_s \; c_s\left(t-\tau\right) e^{j2\pi(f_c+f_d)t} \tag{4}$$

where $\alpha^{(s)}$ is the channel attenuation from the sth satellite to the receiver, τ is the time delay or code phase of the C/A code and f_d is the Doppler frequency for the sth satellite. For this work, S, the total number of satellites is taken as 32.

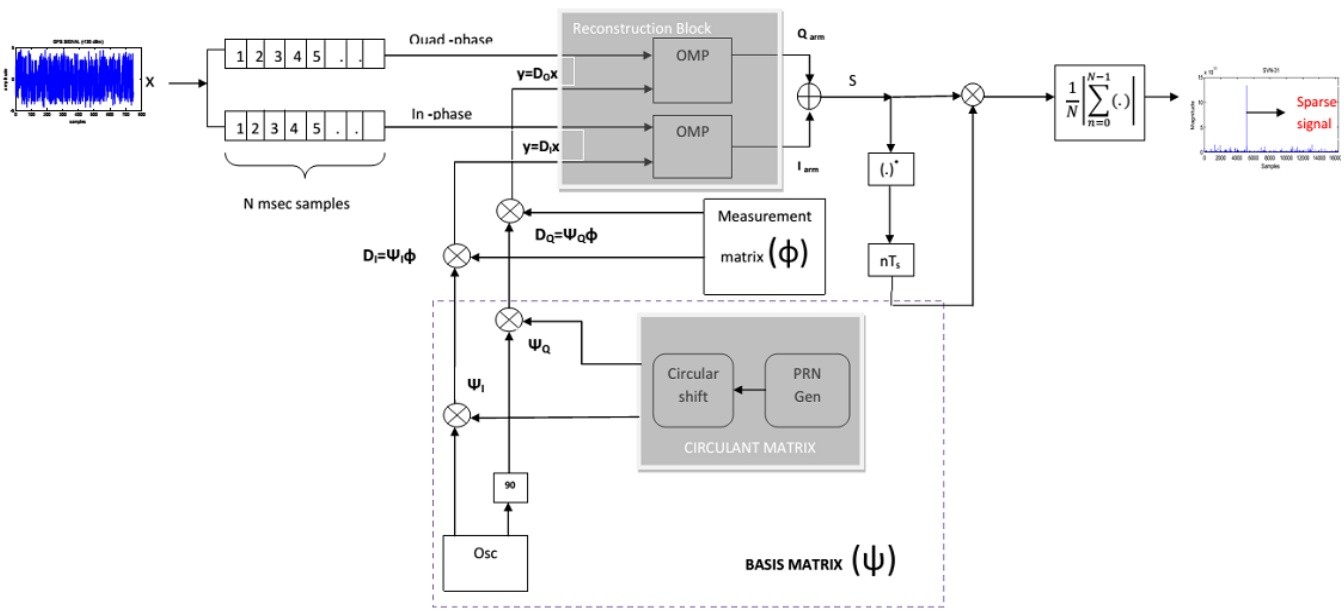

Figure 1: Formulation of GPS sparse signal and its recovery

To decompose the GPS baseband signal into sparse structure, the circular shifted C/A code sequence is multiplied with the corresponding center frequency with Doppler shifts in steps

of 500 Hz for 41 bins (as the Doppler deviation is up to ±10 kHz) for a slow moving receiver. The C/A code is highly orthogonal and thereby the sparsifying basis matrix is created as $\boldsymbol{\psi} \in \dot{\mathbf{R}}^{\mathbf{n}\times(\lambda\times 1023)}$. The C/A code is interpolated with an up sampling factor (λ) to obtain good code precision. The formulated basis ψ is given by

$$\psi = \sum_{i=1}^{32}\sum_{d=1}^{41}\sum_{n=1}^{\lambda*1023}\left[\mathrm{C}\left(\mathrm{n}-\mathrm{N}\right) \bmod \left(\mathrm{N}\right)\right] \times \mathrm{e}^{[\mathrm{j}\times \mathrm{d}\times\Delta\omega(\mathrm{n}-\mathrm{N}) \bmod (\mathrm{N})]} \tag{5}$$

where step size d * 2 π * 500rad/s = 2π *{−10000,−9500, . 0,. . , 9500, 10000} is the set of possible Doppler shifts.

One can perform parallel action of both the operations, namely satellite search (i =1 to 32) and the basis formation (ψ_b) over 41 bins. In this work, iteration over 41 bins with its corresponding basis (ψ_b) is first done, then sequentially the satellite search operation for every basis formation is next performed. The created basis matrix (ψ_b) is multiplied with in-phase and quadrature phase components of a Numerically Controlled Oscillator (NCO) with a carrier frequency of 1.6025 MHz, so that the resultant basis components are ψ_I and ψ_Q respectively. The next step is formation of the measurement matrix (φ) based on the structured matrix as given in [16].

III. A. FORMATION OF KRONECKER PRODUCT OF HYBRID 'L' DETERMINISTIC MEASUREMENT MATRIX

In this work, the measurement matrix is designed based on the Kronecker product of hybrid 'L' matrices for the GPS system and is described as follows. Firstly, a N*N non singular L family matrix is created, in which its non-zero i^{th} originator occurs (2i-1) times, satisfying the condition that, any i^{th} originator is not equal to $(i+1)^{th}$ originator.

$$\phi_L^* = \begin{bmatrix} \varphi_4 & \varphi_3 & \varphi_2 & \varphi_1 \\ \varphi_4 & \varphi_3 & \varphi_2 & \varphi_2 \\ \varphi_4 & \varphi_3 & \varphi_3 & \varphi_3 \\ \varphi_4 & \varphi_4 & \varphi_4 & \varphi_4 \end{bmatrix}$$

This 4*4 matrix is taken as an initial matrix of the measurement matrix. For L- matrices, the condition that the absolute k^{th} row sum is equal to absolute $(n - k + 1)^{th}$ column sum of the matrix should be satisfied as is given as

$$\|\varphi\|_1 = \max_{1\le j\le n}\{\sum_{i=1}^{m}|\varphi_{ij}|\} = \|\varphi\|_\infty = \max_{1\le j\le m}\{\sum_{i=1}^{n}|\varphi_{ij}|\} \tag{6}$$

The L matrices can be formed as a higher dimensional matrix. This higher dimensional matrix is known as hybrid L matrix and the L shape may be regular L, reverse L, inverted L and reverse inverted L. The combination of these four type L shape in any order can be written as

$$\phi_L = \begin{bmatrix} \phi_L^* & \phi_L^* & \phi_L^* & 0 \\ \phi_L^* & 0 & \phi_L^* & \phi_L^* \\ \phi_L^* & \phi_L^* & 0 & \phi_L^* \\ 0 & \phi_L^* & \phi_L^* & \phi_L^* \end{bmatrix}$$

In the next step, block L matrix is constructed by enlarging ϕ_L into a bigger size matrix of order greater than the previous matrix in which the matrix has the same building block.

$$\phi_L^{'} = \begin{bmatrix} \varphi_L & 0 \\ \varphi_L & \varphi_L \end{bmatrix}$$

Similarly, the next block L matrix has been determined by finding $\phi_L^{'}, \phi_L^{''}, ...\phi_L^{p}$.

$$\phi_L^{''} = \begin{bmatrix} \varphi_L^{'} & 0 \\ \varphi_L^{'} & \varphi_L^{'} \end{bmatrix}$$

$$\vdots$$

$$\phi_L^{p} = \begin{bmatrix} \varphi_L^{p-1} & 0 \\ \varphi_L^{p-1} & \varphi_L^{p-1} \end{bmatrix}$$

Finally, the Kronecker products of p= $\log_2 N$ matrices give the measurement matrix with N*N required elements.

$$\phi = \phi_L \otimes \phi_L^{'} \otimes \phi_L^{''} \otimes \phi_L^{'''} \ldots \quad \ldots. \otimes \phi_L^{p} \tag{7}$$

After formulating this matrix, it is essential to find the rotation matrix i.e., nearest orthonormal matrix to satisfy the singleton bound and mutual coherence between the columns of the matrix. So, from the given matrix φ the matrix φ^r is found such that it minimizes $\| \varphi - \varphi^r \|^2_F$ subject to $(\varphi)^T\varphi^r = I$. By introducing a symmetric Lagrangian multiplier matrix μ, the orthogonality constraint has been achieved.

$$e(\varphi^r, \mu) = ((Trace(\varphi - \varphi^r)^T(\varphi - \varphi^r)) + Trace(\mu(\varphi^r)^T\varphi^r - I)) \tag{8}$$

Differentiating $e(\varphi^r, \mu)$ w.r.to φ^r and equating the result to zero yields

$$\varphi = \varphi^r(I + \mu) \tag{9}$$

Thus from (9) , the measurement matrix is decomposed into a product of an orthonormal and asymmetric matrix.

$$(\varphi)^T\varphi = (\mathrm{I} + \mu)(\varphi^r)^T\varphi^r(\mathrm{I} + \mu) = (I + \mu)^2 \tag{10}$$

Hence, $(\mathrm{I} + \mu) = \sqrt{\varphi^T\varphi}$

$$\varphi^r = \varphi(\mathrm{I} + \mu)^{-1} = \frac{\varphi}{\sqrt{\varphi^T\varphi}} \tag{11}$$

The inverse square root of $(\varphi^T\varphi)$ is calculated by eigen value eigen vector decomposition

$$\sqrt{\varphi^T\varphi} = \frac{1}{\sqrt{\sigma_1}}\mathrm{e}_1\mathrm{e}_1{}^{\mathrm{T}} + \frac{1}{\sqrt{\sigma_2}}\mathrm{e}_2\mathrm{e}_2{}^{\mathrm{T}} + \cdots\frac{1}{\sqrt{\sigma_n}}\mathrm{e}_n\mathrm{e}_n{}^{\mathrm{T}} \tag{12}$$

III. B. RECOVERY OF SPARSE SPIKE

The measurement matrix (φ^r) designed based on the Kronecker product of hybrid 'L' matrices is multiplied with the in-phase and quadrature basis $\psi_I\phi^r$ and $\psi_Q\phi^r$ which are known as dictionary matrices D_I and D_Q respectively. The compressed measurements are given by

$$y = \varphi^r\psi s \tag{13}$$

$$\mathrm{y}^{(\mathrm{i,d,n})}(\mathrm{n}) = \sum_{i=1}^{32}\sum_{d=1}^{41}\sum_{n=1}^{\lambda*1023} \mathrm{D}(\mathrm{n}) \times \mathrm{S}^{(\mathrm{i,d,n})}(\mathrm{n}) \tag{14}$$

where $D(n) = \psi\varphi^r = \left[\mathrm{C}(\mathrm{n} - \mathrm{N}) \bmod (\mathrm{N})\right] \mathrm{e}^{[\mathrm{j}\times\mathrm{d}\times\Delta\omega(\mathrm{n}-\mathrm{N}) \bmod (\mathrm{N})]} \times \varphi^r$, $\mathrm{S}^{(\mathrm{i,d,n})}(\mathrm{n})$ is the amplitude of the sparse peak associated with the satellite, Doppler shift and code phase which makes the signal have a sparse representation.

Finally the compressed measurements $y_I = \Phi^r{}_I X_I = Ds_I$, and $y_Q = \Phi^r{}_Q X_Q = Ds_Q$ with a size of M × N and the signal vector (x) of size M × 1 are given as an inputs to Orthogonal Matching Pursuit (OMP) algorithm to obtain the recovered in-phase and quadrature signals.

$$\mathrm{y}_I{}^{(\mathrm{i,d,n})}(\mathrm{n}) = \sum_{i=1}^{32}\sum_{d=1}^{41}\sum_{n=1}^{\lambda*1023} \mathrm{D}_I(\mathrm{n}) \times \mathrm{S}_I{}^{(\mathrm{i,d,n})}(\mathrm{n}) \tag{15}$$

$$\mathrm{y}_Q{}^{(\mathrm{i,d,n})}(\mathrm{n}) = \sum_{i=1}^{32}\sum_{d=1}^{41}\sum_{n=1}^{\lambda*1023} \mathrm{D}_Q(\mathrm{n}) \times \mathrm{S}_Q{}^{(\mathrm{i,d,n})}(\mathrm{n}) \tag{16}$$

The sparse spike peak (S) is obtained by taking the magnitude value of the reconstructed sparse $\mathrm{S}_{\mathrm{I}}{}^{(\mathrm{i,d,n})}$ and $\mathrm{S}_{\mathrm{Q}}{}^{(\mathrm{i,d,n})}$ vectors.

$$Sparse^{(i,d,n)} = \left| S_I^{(i,d,n)} + jS_Q^{(i,d,n)} \right| \tag{17}$$

The sparse spike output of the OMP algorithm is further fed in to the differential coherent detection block and the dominant spike (S) after 'k' integration times of differential combining for 32 satellites and calculated sequentially as

$$s = \sum_{i=1}^{k} s_I s_{I-1}{}^* + s_Q s_{Q-1}{}^* = \left\{ sparse^{(0,0,0)}, sparse^{(0,0,1)} \cdots sparse^{(32,41,\lambda\times 1023)} \right\} \tag{18}$$

As per the Kronecker product measurement matrix design, it should satisfy the two important properties namely Mutual coherence and Restricted Isometry.

a. Mutual coherence property

The coherence of a matrix (φ) is the largest absolute inner product between any two columns of φ is given by as in [17]

$$\mu(\varphi) = \max_{1\le i\ne j\le N} \frac{|\langle \varphi_i | \varphi_j \rangle|}{\|\varphi_i\|_2 \|\varphi_j\|_2} \tag{19}$$

To efficiently represent the sparse signal, the inner product of two columns should be incoherent and the value of coherence should be very small i.e. $\mu(\varphi) \in \left[\sqrt{\frac{N-M}{M(N-1),}}, 1 \right]$. The l_1-norm minimal solution has a faithful reconstruction of a sparse signal if and only if $k \le \frac{\left[1+\frac{\mu(\varphi)}{2}\right]}{2}$.

If the measurement matrix is considered to be Kronecker product of matrices $\varphi_1, \varphi_2, \cdots \varphi_p$, then the condition for mutual coherence is as in [17]

$$\mu(\varphi_1 \otimes \varphi_2 \otimes \varphi_3 \cdots \otimes \varphi_p) = max\{\mu(\varphi_1), \mu(\varphi_2), \mu(\varphi_3), \cdots \mu(\varphi_p)\} \tag{20}$$

b. Restricted Isometry property (RIP)

If a measurement matrix (φ) satisfies the equation $(1-\delta_K)\|s\|_2^2 \le \|\varphi\psi s\|_2 \le (1+\delta_K)\|s\|_2^2$ for all possible k-sparse vectors 's' with smallest nonnegative number $0 \le \delta_k < 1$, then φ is said to obey the Restricted Isometry property with restricted isometry constant δ_k. Suppose the

Kronecker product matrices $\varphi_i \in R^{m,n}$ having with normalized columns $(\varphi_1 \otimes \varphi_2 \otimes \varphi_3 \cdots \otimes \varphi_p)$ then, the RIP condition for Kronecker product is given as [17]

$$\delta_k{}^{(\varphi_1 \otimes \varphi_2 \otimes \varphi_3 \cdots \otimes \varphi_p)} \ge max\{\delta_k{}^{\varphi_i}\} \text{ for } 1 \le i \le p. \tag{21}$$

III. C. OMP ALGORITHM FOR SPARSE SPIKE PEAK RECOVERY

Input: Dictionary matrix D_I, D_Q ; measurement vector y_I, y_Q

Output: Sparse vector S_I and S_Q (32×41×λ*1023)

Step 1: Initialize the residual r_0= $\mathbf{y_I}$ and initialize the set of selected variable $\mathbf{D_I}$ =Φ. Let the iteration counter n = 1.

Step 2: Determine the index I_{max} by taking the maximum correlation between the measurement matrix and residue

Step 3: Update the set $g^n = g^{n-1} \cup \{I_{max}\}$.

Step 4: Determine the estimated signal s^n using least squares method

Step 5: Calculate the new residual r^n

Step 6: If the residual is less than minimum error bound, stop the algorithm, otherwise, increment the iteration counter.

Step 7: Repeat steps 1 to 6 for quadrature phase input **(y_Q, D_Q)**

IV. SIMULATION RESULTS

The digitized input sample data length of 5714 with a centre frequency 1.6025 MHz is used for simulation. The compressed sensing based GPS signal acquisition has been performed under the signal power level of 25 dB-Hz. The decision statistic which crosses the specified threshold value has been determined for three different longer duration detection schemes. The performance of the acquisition with compressed to uncompressed data, comparison of different measurement matrices used in compressed sensing based acquisition and their computation time are calculated.

a. Acquisition of GPS satellites using compressed longer duration data

The number of measurements (m) plays a crucial role in recovering the sparse signal. If the signal is represented as 'k' sparse then the number of measurements required to faithfully reconstruct the signal is given as $m \geq c \times k \times log\left(\frac{N}{k}\right)$ where c is positive constant and N refers to length of the signal [1]. Based on this condition, the number of measurements should be carefully chosen to identify the robust peak. Initially, the compression factor is set as 0.10 with chunk length 1

msec. It is observed that, for good recovery of sparse spike signal around 35dB-Hz with nominal amount of false alarm, single msec data is sufficient. However, for a 25dB-Hz weak signal, it does not pick the robust spike. Even after increasing the compression factor from 0.1 to 0.4, the single msec data fails to precede the acquisition process.

A longer duration data (1-20 msec) is next used for the simulation. By extending the period for processing the weak signal, the ability to spot the sparse signal is more compared to the single msec duration data. The number of visible satellites is plotted in figure 2 for three post correlation detection techniques namely coherent, non-coherent and differential coherent detection. However, the first two detection methods fail to satisfy the necessity of four satellites to find out the user position. Only one satellite was found by keeping k=20 and M/N= (0.1 - 0.5). Since, data transition problems occur in coherent detection, length of the data cannot be extended beyond 20 msec. In the case of non-coherent detection up to 100 msec, only three satellites are visible even after increasing the compression factor 0.6. If the data length is increased beyond 100 msec, there is a possibility of finding a sparse spike but the mean acquisition time exceeds the time to first position fix, thereby decreasing the acquisition sensitivity.

The differential coherent (DC) detection requires accumulation after ‘k’ difference making the requirement of the accumulation algorithm time shorter, and the frequency difference intolerance higher. Hence the optimal choice of fixing the compression factor and data length using DC improves the decision statistic. By combining k=20 one msec differential detection chunks and M/N=0.4, the exact recovery of peak index i.e., code phase is found for four satellites. On the other hand, in the coherent and non-coherent detection methods, the ratio of the first to the second tallest peak is more and the location of dominant peak i.e. the code phase deviation is more which leads to incorrect recovery of a satellite.

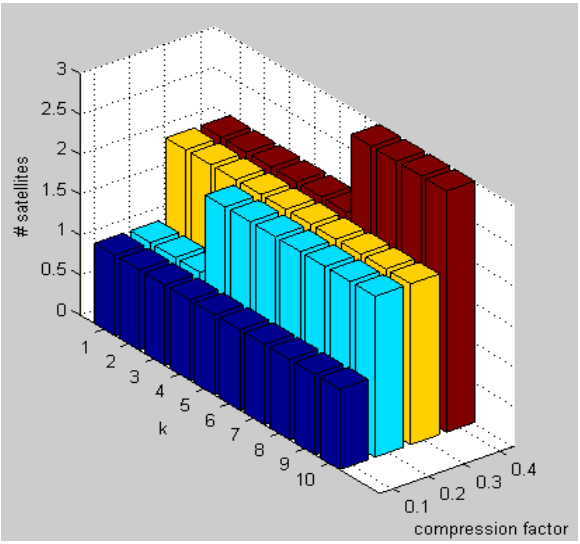

(a)

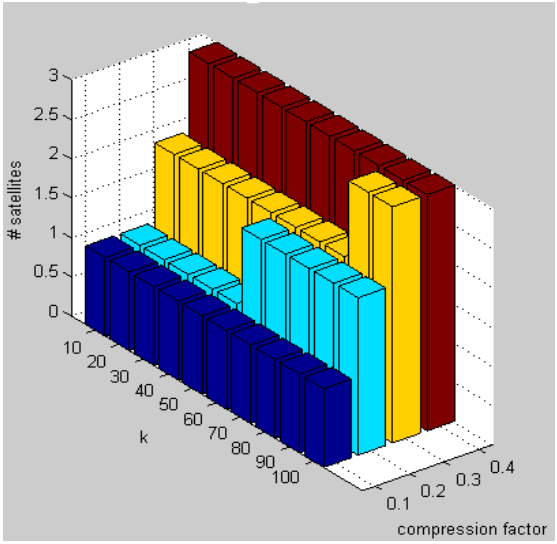

(b)

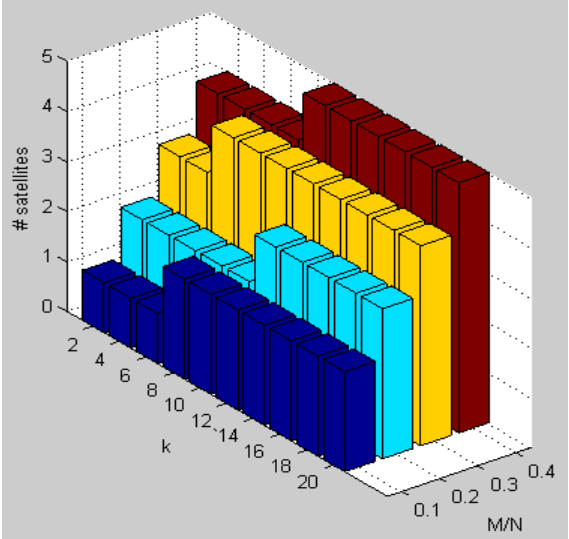

(c)

(a) Coherent (b) Non-coherent (c) Differential coherent

Figure 2: Satellites in view for different compression factors using longer duration data of 1-20 msec

The acquisition result of four SVN's 1,4,15 and 29 for four detection types are plotted in figure 3a, 3b, 3c and 3d respectively.

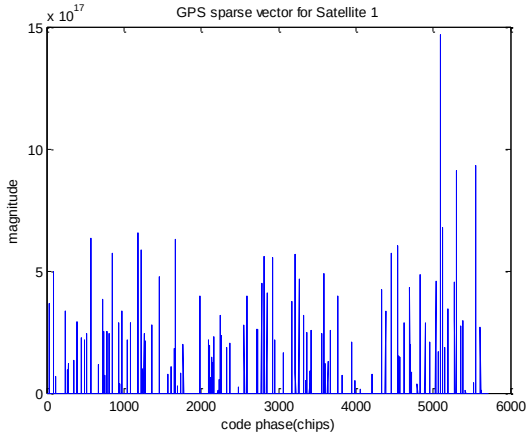

(i)

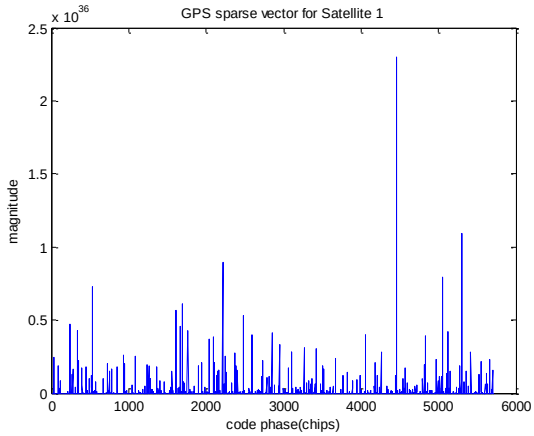

(ii)

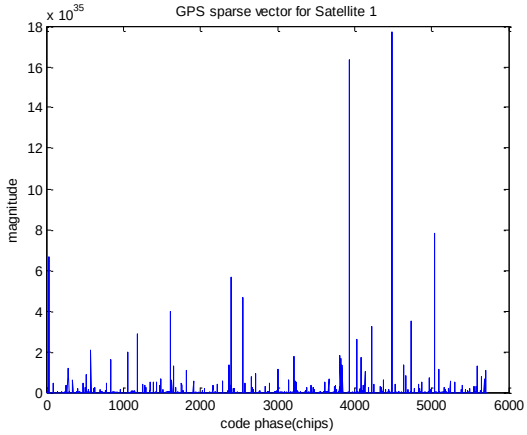

(iii)

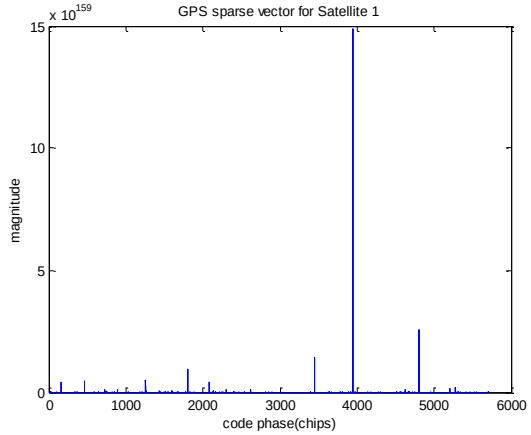

(iv)

(i) Single msec data (ii) Coherent detection (iii) Non- coherent detection (iv) differential coherent detection

Figure 3.a: Visible SVN-1

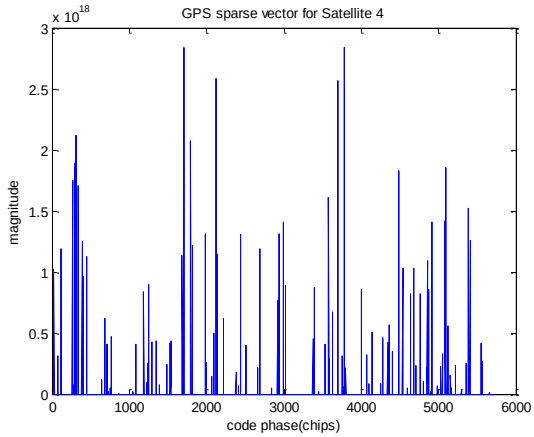

(i)

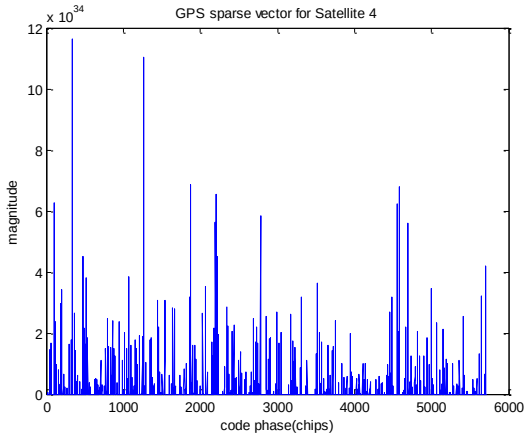

(ii)

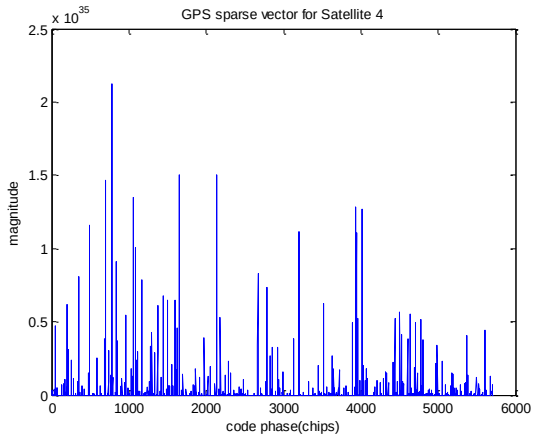

(iii)

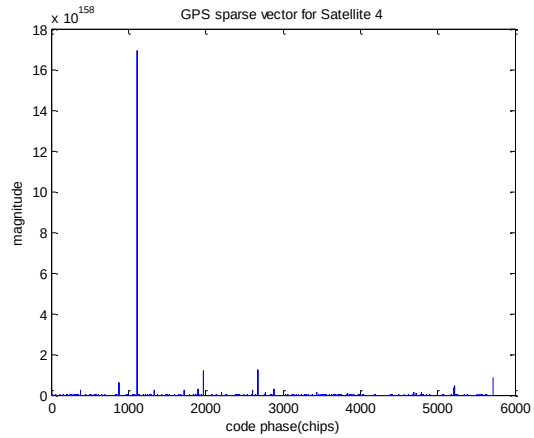

(iv)

(i) Single msec data (ii) Coherent detection (iii) Non- coherent detection (iv) Differential coherent detection

Figure 3.b: Visible SVN- 4

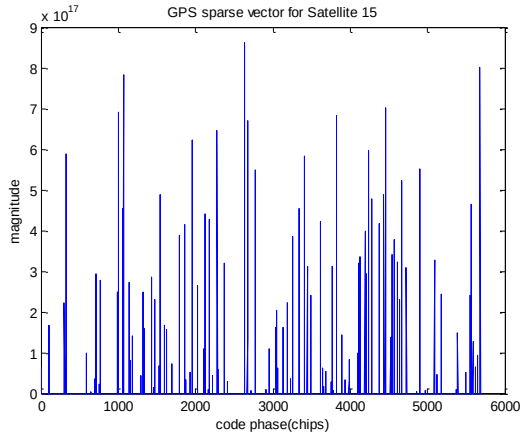

(i)

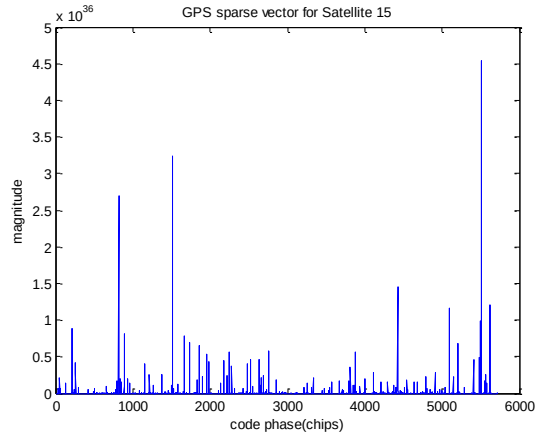

(ii)

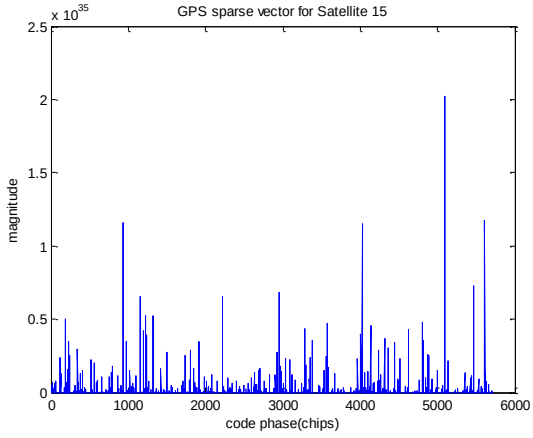

(iii)

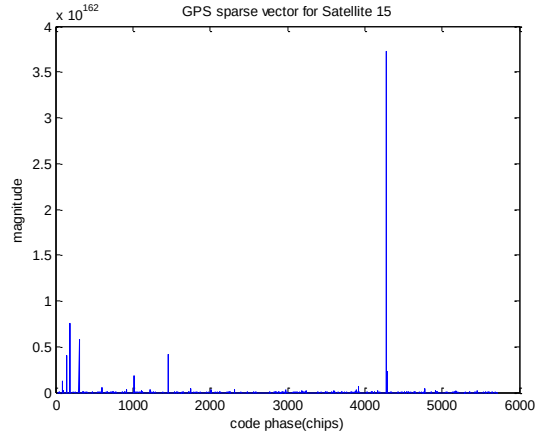

(iv)

(i) Single msec data (ii) Coherent detection (iii) Non- coherent detection (iv) Differential coherent detection

Figure 3.c: Visible SVN- 15

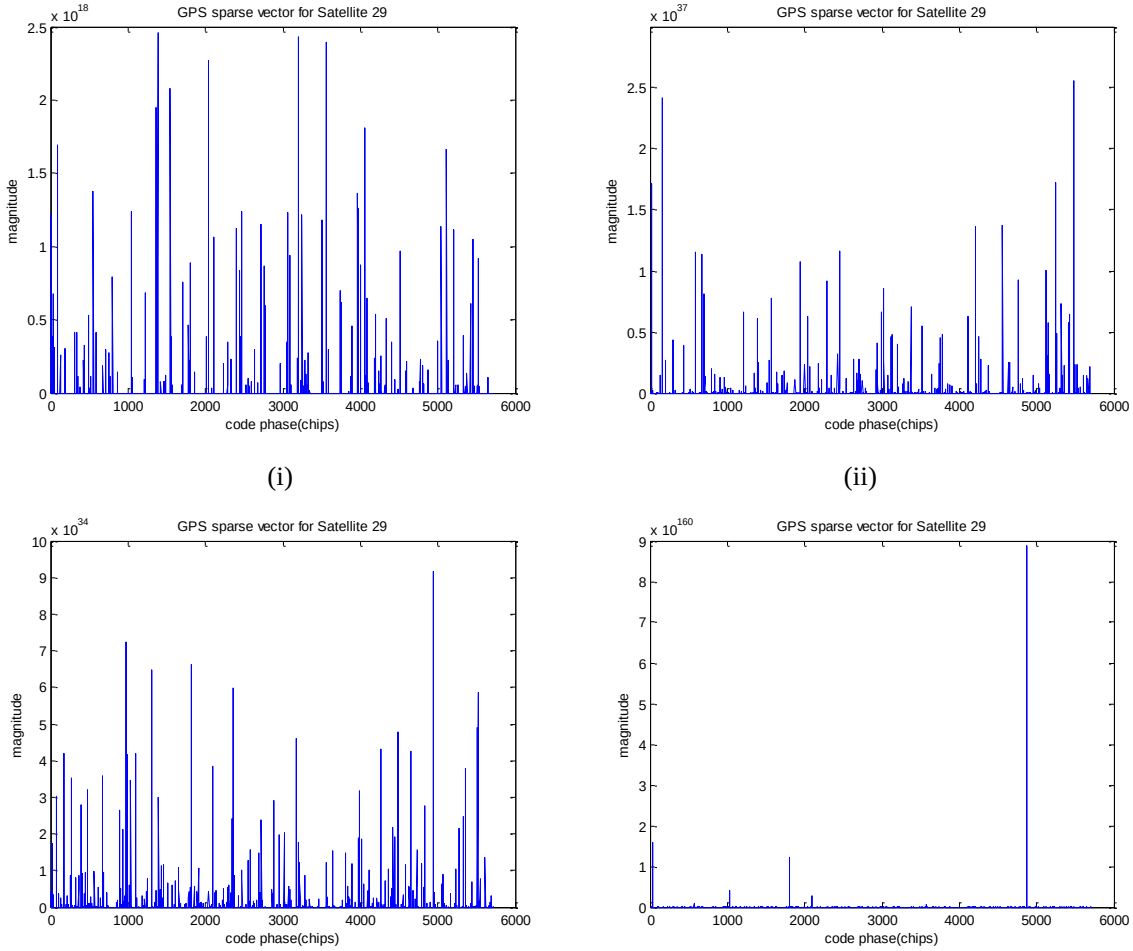

(i) Single msec data (ii) Coherent detection (iii) Non- coherent detection (iv) Differential coherent detection

Figure 3.d: Visible SVN-29

Figure 4 shows the performance evaluation of the four detection types using the Receiver's Operating Characteristic (ROC). The Figure 4 depicts the ROC plot of SVN 29 under the signal range 25 dB-Hz. The differential detection has the highest detection probability compared to other detection schemes and is identified as the best performing detector which has the minimum distance from the ideal point (Probability of detection, P_d = 1 and Probability of false alarm, P_{fa}= 0) in the ROC curve.

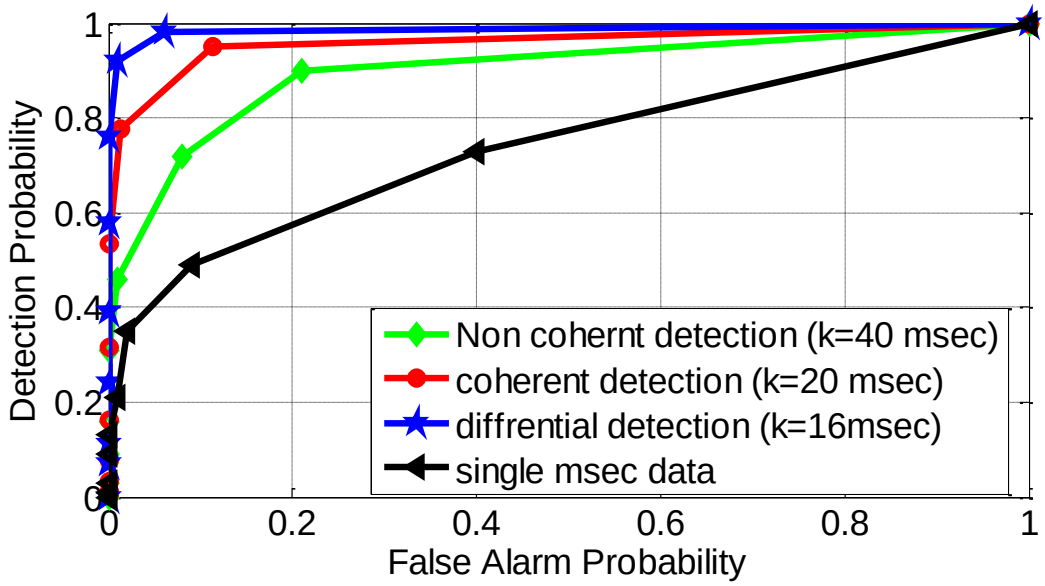

Figure 4: ROC plot for different detection schemes

b. GPS Acquisition sensitivity analysis of compressed to uncompressed data length

While fixing the optimal value of compressed measurements (M/N) and data length (k), it is observed that there is a tradeoff in satellite count between using compressed data length [(M/N)*k] msec to uncompressed data length (k msec). If the performance of the both the cases are equal then the ratio $\frac{(\frac{M}{N} * k)}{k}$ is nearly equal to one. Table 1 shows the value of the ratio of compressed to uncompressed data length in terms of number of visible satellites for the three detection methods.

From Table 1, it is observed that the highest ratio of 0.9 is achieved only in differential detection scheme. Even a nominal value has not been achieved by the other two detection schemes with various compression factors and data lengths. Referring to the last row in the Table 1, in differential detection method, to process a 25 dB-Hz weak signal, fixing M/N=0.4 and k= (16-20) results in 1-2 visible satellite lesser than its uncompressed 16-20 msec segment. This smaller variation within the satellite visibility does not have an effect on the acquisition quality since the minimum requirement of four visible satellite count has been met in both the cases. However, processing (0.4*20) × 8 msec data requires 45,712 samples while its uncompressed data (20 msec) requires 1,14,280 samples. Though the uncompressed data provides the additional 1-2 satellite count; but the larger number of samples only slows the acquisition speed.

The percentage of reduction in samples is calculated as [1-compressed data length / uncompressed data length]×100%. Using the CS approach, instead of using 20×5714=1,14,280 samples, one can use only 0.4×20×5714 =45,712 samples resulting in a reduction of 60 % data length.

Table 1. Ratio of the visible satellites for three detection methods

Detection type	**Compressed measurement (M/N)**	**Data length (k)**	**Ratio =** $\frac{(M/N * k)}{k}$
Coherent	0.1	2-20	0.2
	0.2	2-20	0.3
	0.3	2-20	0.3
	0.4	2-20	0.4
Non coherent	0.1	2-20	0.3
	0.2	20-50	0.4
	0.3	50-100	0.5
	0.4	>100	0.6
Differential coherent	0.1	5-20	0.6
	0.2	10-20	0.6
	0.3	12-20	0.8
	0.4	16-20	0.9

Conversely, if we analyze the compressed data length to its absolute or uncompressed data length, the compressed data results in good performance than the uncompressed equivalent data length i.e., when M/N=0.4 and k=20 (8 msec data length) provides 92% probability of obtaining 1.2 times more number of visible satellites than their uncompressed absolute data length of 8 msec. The performance comparison of compressed to absolute data length is shown in figure 4.

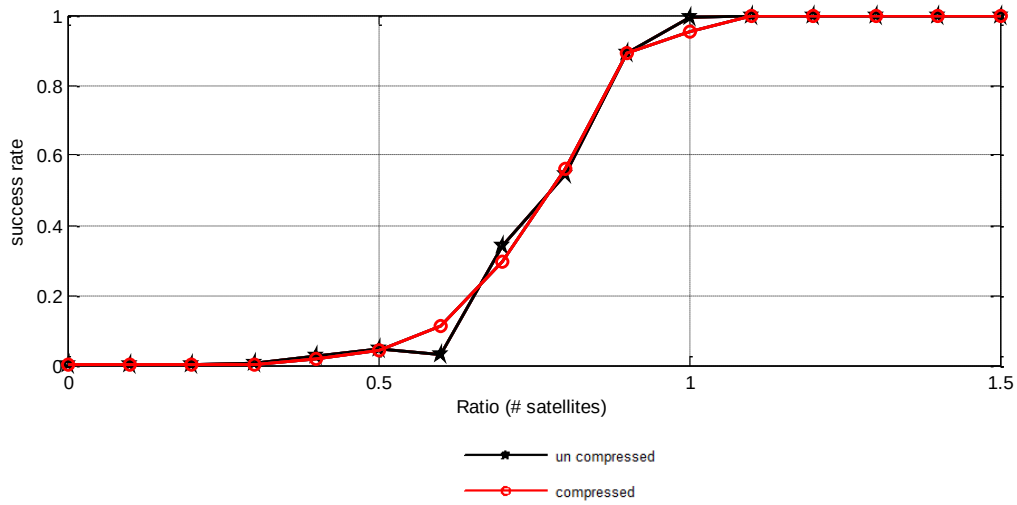

Figure 4: Performance of compressed to uncompressed absolute data length

c .Performance comparison of different measurement matrices used in GPS acquisition

The performance comparison of various types of measurement matrices including random, Bernoulli, binary measurement and Kronecker product of L matrix have been carried out in the acquisition stage. Monte Carlo simulation for GPS acquisition was used and the success rate was calculated. Success rate is defined as the average number of times the peaks crosses the threshold values and is given by equation (22)

$$sucess\ rate = \frac{\text{number of times the peak crossed the threshold}}{\text{Number of trails}} \times 100 \qquad (22)$$

As per the peak condition, the difference between maximum, mean peak values and difference between 1st maximum and 2nd maximum peak values should be greater than 0.3 and 0.15 respectively. In order to get a minimum probability of false alarm 10^{-2}, the threshold values are chosen as 0.99 and 0.25 respectively and the number of trails is set as 5000 for each compression factor.

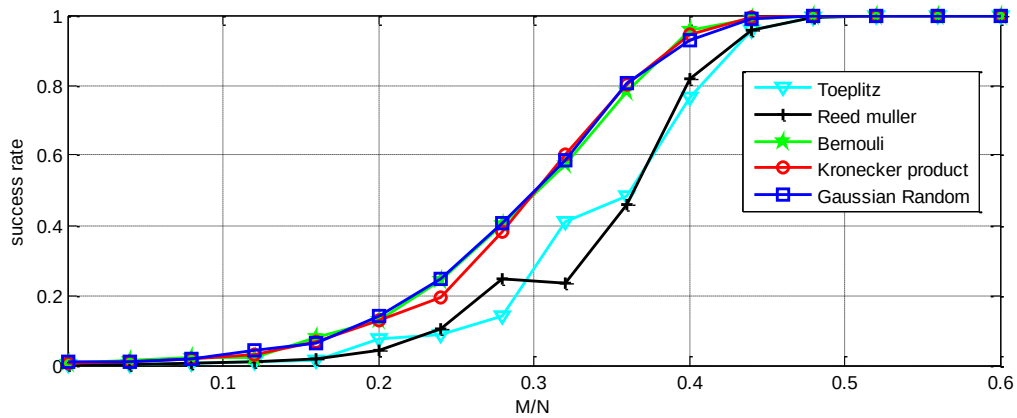

Figure 5: Compression factor (M/N) versus success rate for different measurement matrices

From figure 5, it is evident that the Gaussian random and Bernoulli matrices attain 95% success rate at a compression factor of 0.4 and k=20. Similarly the proposed measurement matrix using Kronecker product of L matrix also performs equivalently well. However, in the case of the Toeplitz and Reed Muller matrices, the detection of correct peak is found as 78% and 80% respectively. If the compression factor is increased by 0.5 and k=18, all the matrices produce 100% correct identity of satellite but the number of required samples would be around 51,426 which decreases the acquisition speed. Hence, the compressing factor is fixed at 0.4 using proposed Kronecker product of L matrix measurement matrix having 45,712 samples with 11% reduction of data length in order to speed up the acquisition process.

d. SNR performance comparison of different measurement matrices used in GPS acquisition

The SNR performance of the proposed method is studied in this section. The SNR computation in the software receiver is calculated as the ratio between the accumulated and averaged in phase arm ($\hat{I}_{arm}$) power to the accumulated and averaged noise power ($\hat{Q}_{arm}$) given by equation as in [18]

$$SNR = 10log_{10}\left(\frac{\hat{I}_{arm}{}^2}{2\hat{Q}_{arm}{}^2}\right)dB \tag{23}$$

$$\hat{I}_{arm}{}^2 = \frac{(f_s\tau)^2 c}{2} \text{ and } \hat{Q}_{arm}{}^2 = f_s\tau\sigma_y{}^2$$

where τ is Integration time, C is carrier power and $\sigma_y{}^2$ is the noise variance

Table 2 gives the comparison of post-correlation SNR values computed for different measurement matrices. The received GPS signal with signal level of 25 dB-Hz has been processed and its post correlation SNR for all visible satellites are calculated using eqn (23).To measure the SNR value of visible satellites, the incoming signal is correlated with the locally generated 32 PRN codes with 'k' times differential accumulation of compressed sensing adopted acquisition process, and only 4 SVNs (1, 4, 15 and 29) cross the threshold.

Table 2. Comparison of post-correlation SNR values of the different measurement matrices

SVN	Gaussian Random (dB)	Circulant Toeplitz (dB)	Reed Muller (dB)	Bernoulli (dB)	Kronecker product (dB)
1	11.89	10.45	10.64	11.33	11.16
4	13.09	11.32	11.57	12.26	12.11
15	11.08	9.89	9.61	10.47	10.26
29	12.7	11.01	10.46	12.05	11.96

From Table 2, it is inferred that the Gaussian random measurement matrix performs better with highest SNR values of 11.89, 13.09, 11.08 and 12.7 dB respectively for 4 SVN's. The Bernoulli matrix also equivalently perform well with an average marginal difference of 0.57 dB with respect to random matrix. However, both the matices are generated based on certain distributions. Due to this, a special library function has to be called for its implementation in embedded hardware. On the other hand, while testing the deterministic family of measurement matrices namely Kronecker, Reed Muller and Circulant Toeplitz, a small relative difference in average SNR of 0.84dB is achieved using Kronecker product matrix with respect to Gaussian Random matrix but, for the latter two matrices, the average SNR difference is around 1.62 dB and 1.49 dB which is more than 1 dB. From this result, it is clear that the Kronecker product is suitable for improving the SNR of the weak GPS signal. Another important observation is that by increasing

the number of measurements, the SNR value increases but the percentage of reduction in sample decreases.

e. Computation Time

In order to validate the computation complexity of the Compressed Sensing based acquisition process, the computation time required to obtain first position fix was calculated. The execution time is calculated on a 1.46 GHz processor with 1 GB memory using MATLAB software. Table 3 shows the comparison of the computation time. It can be seen that all the exisitng sensing matrices take higher computation time and the Kronecker product determines the sparse spike faster within a very shorter period 10.41 sec. Thus using the Kronecker product, the acquisition process is accelerated and reacquisition is avoided by combining it with the differential compressed detection scheme.

Table 3. Comparison of Computation Time

Type of measurement matrix	Execution time (sec)
Gaussian Random	28.74
Bernoulli	26.53
Circulant Toeplitz	16.67
Reed Muller	18.34
Kronecker product	10.41

V. CONCLUSION

In this paper, weak GPS signal acquisition is implemented by adopting Compressed Sensing approach. From the simulation results, it is evident that the sparse signal processing combined compressed differential post correlation detection improves the acquisition sensitivity in terms of lesser computation time and reduction in number of samples when compared to traditional serial and parallel code phase search schemes. Using CS approach, a reduction of 60 % data length is achieved with 8 msec compressed measurement rather than utilizing 20 msec data segment. Moreover, the compressed data obtained by fixing compression factor (M/N) of 0.4 and k equal to 20 msec differential detection achieves 1.2 times more number of visible satellites than its uncompressed equivalent absolute data length. The proposed Kronecker product of hybrid L

measurement matrix has superior performance as it diminishes the data length by 11% with 10.41 sec shorter mean acquisition time when compared to Reed Muller and Circulant Toeplitz measurement matrices. In addition, using the proposed technique, the SNR of the visible satellite's peak autocorrelation function has also improved compared to existing schemes.

REFERENCES

[1] E.J. Candès, J. Romberg, T. Tao, Robust uncertainty principles: exact signal reconstruction from highly incomplete frequency information, IEEE Trans. Inform. Theory 52 (2) (2006) 489–509.

[2] Xiao Li, Andrea Rueetsch, Yonina C. Eldar, Anna Scaglione, GPS signal acquisition via compressive multichannel sampling, Physical Communication 5 (2012) 173–184

[3] T. L. Hansen, D. H. Johansen, P. B. Jørgensen,K. F. Trillingsgaard, T. Arildsen, K. Fyhn and T. Larsen , Compressed Sensing with Rank Deficient Dictionaries, IEEE Globecom 2012.

[4] Ihsan Alshahib Lami, Ali Albu-Rghaif, Maher Al-Aboodi, GCSR: A GPS Acquisition Technique using Compressive Sensing enhanced implementation, International Journal of Engineering and Innovative Technology ,Vol. 3, Issue 5, 2013.

[5] Halder, T.; Bhattacharya, A., "Weak GNSS signal acquisition using prolate spheroid wave function based compressive sensing," in Students' Technology Symposium (TechSym), 2014 IEEE , vol., no., pp.233-238.

[6] Prasant Kumar Misra, Wen Hu, Yuzhe Jin, Jie Liu, Amanda Souza de Paula, Niklas Wirstrom, and Thiemo Voigt. 2014. Energy efficient GPS acquisition with sparse-gps. In Proceedings of the 13th international symposium on Information processing in sensor networks (IPSN '14). IEEE Press, Piscataway, NJ, USA, 155-166.

[7] Ying Xiao, Wanlin Gao, Ganghong Zhang, and Han Zhang, "Compressed Sensing Based Apple Image Measurement Matrix Selection," International Journal of Distributed Sensor Networks, vol. 2015, Article ID 901073.

[8] Vibha Tiwari, P.P. Bansod & Abhay Kumar, Designing sparse sensing matrix for compressive sensing to reconstruct high resolution medical images, Cogent Engineering (2015), 1017244.

[9] Zhang, Xiang Tong, Wei Wang and Jiazu Xie, The research of Kronecker product based measurement matrix of compressive sensing, EURASIP Journal on Wireless Communications and Networking, 2013:161.

[10] Sabna N, P.R.Saseendran Pillai, Matrix Padding Method for Sparse Signal Reconstruction, Signal Processing: An International Journal (SPIJ), Vol. 9, Issue -1, pp 1-13.

[11] Desai and Nakrami Kezhi , Improved Performance of Compressive Sensing for Speech Signal with Orthogonal Symmetric Toeplitz Matrix, International Journal of Signal Processing, Image Processing and Pattern Recognition,Vol.7, No.4 (2014), pp.371-380.

[12] Aasha Nandhini Sukumaran Radha Sankararajan, Kishore Rajendiran. Video Compressed Sensing framework for Wireless Multimedia Sensor Networks using a combination of multiple matrices. Comput Electr Eng (2015).

[13] D.L. Donoho, Compressed sensing, IEEE Trans. Inform. Theory 52 (4) (2006) 1289–1306E.J. Candès, T. Tao, Decoding by linear programming, IEEE Trans. Inform. Theory 51 (12) (2005) 4203–4215

[14] Candès Emmanuel J, Wakin Michael B. An introduction to compressive sampling. IEEE Signal Process Mag 2008;25(2):21–30

[15] Michel S.Braasch, A.J Van Dierendonck, GPS Receiver architecture and measurements, Proceedings of the IEEE, vol no.87, 1999, pp.48-64.

[16] Rahul Gupta, Garimella Rama Murthy, Innovative Structured Matrices, Advances in Linear Algebra & Matrix Theory, 2013, 3, pp.17-21

[17] Sadegh Jokar, Volker Mehrmann, Sparse solutions to underdetermined Kronecker product systems, Linear Algebra and its Applications 431 (2009) 2437–2447.

[18] Angelo Joseph, Measuring GNSS Signal strength, Inside GNSS Magazine, November/December 2010, pp.20-25.